Human Facial Image Age Group Classification Based On Third Order Four Pixel Pattern (TOFP) of Wavelet Image

Rajendra Chikkala[1], Sreenivasa Edara[2], and Prabhakara Bhima[3]
[1]Department of Computer Science and Engineering, Research Scholar, India
[2]Department of Computer Science and Engineering, Dean Acharya Nagarjuna University College of Engineering and Technology, India
[3]Department of Electronics and Communication Engineering, Jawaharlal Nehru Technological University Kakinada, India

Abstract: *The present paper proposes a novel scheme for age group classification based on Third Order Four pixel Pattern (TOFP). This paper identified TOFP patterns in two forms of diamond pattern which have four pixels i.e., outer diamond and inner diamond patterns in Third Order neighborhood. The paper derives Grey-Level Co-occurrence Matrix (GLCM) of a Wavelet image based on the values of Outer Diamond Corner Pixels (ODCP) of TOFP and Inner Diamond Corner Pixels (IDCP) of TOFP on wavelet image which is generated from the original image without using the standard method for generating the co-occurrence matrix. Four GLCM features are extracted from the generated matrix. Based on these feature values, the age group of the human facial image was categorized. In this paper, human age is classified into six age groups such as Child: 0-9 years, Adolescent: 10-19 years, Young Adult: 20-35 years, Middle-Aged Adults: 36 -45 years, Senior Adults 46–60 years, Senior Citizen: age > 60. The proposed method is tested on different databases and comparative results are given.*

Keywords: *GLCM, pixel pattern, age group classification, four pixel pattern, outer diamond, inner diamond.*

Received July 23, 2015; accepted March 24, 2016

1. Introduction

In the area of computerized analysis of facial images for recognition, ethnicity classification, gender recognition etc. the age estimation is a barely explored part. However, in the recent times, the interest in this subject has significantly increased because of its many practical applications. For example, there are age limitations for driving a car, buying alcohol, use of cigarette-vending machine for under-aged people, face-recognition robust to age progression, an internet access control, films watching, video games age-based retrieval of face images and age prediction systems for finding lost children. In addition, the estimated age of consumers who look at billboards is used in age specific target advertising as consumer preferences differ greatly by age which fact should be accepted, but the human skill of age estimation is very limited. So, a computer system which supports the persons responsible would be helpful. It is well known that the human-computer interaction varies for different age groups. Thus a system which automatically adapts its interface to the age of the current user would clear this problem. Unfortunately, age classification itself is an extremely difficult task because of the continuous changes in the cranio-facial district, the skinny portion of the head and the overlying delicate tissue created by the maturing advancement [25]. Geng *et al*. [7] built up an age prediction technique named Aging pattern Subspace (AGES), based on the following assumptions:

- The aging development is unmanageable.
- Every person ages differently.
- The aging growth must follow the organize of time.

Therefore they introduced aging patterns, as a succession of individual facial images variety in chronological arrangement. The images are represented by their feature vector, extracted by the Appearance Model described in [4]. To maintain verification/identification performance in the age variation, some researchers have challenged to address this issue of categorizing the subject's age [3, 5]. The feature extraction can be divided into three steps: the age group categorization [6, 12, 17, 21], the single-level age assessment [8, 19, 20, 26, 29] and the hierarchical age assessment [9, 19, 22]. Burt and Perrett [2] developed blended faces for altered age groups by accretion the boilerplate appearance and arrangement of animal faces that accord to anniversary age group. This adjustment allocates facial into three categories and the allocation ante for anniversary ambit were about 63.5%, 69.8% and 61.5%. Lanitis *et*

al. [20] compared the parametric archetypal age admiration action with that of neural networks based approaches to allocate the angel into four classes. The boilerplate age accumulation allocation amount is about 69.7%.

Every input image is contrasted with age pattern which got hold to the age estimation result. Horng *et al*. [12] measured four age classes for arrangement, the classes being infants, young, middle-aged, and senior citizens. Their methodology [12] was partitioned into three stages: area, highlight extraction, and age grouping. In view of the harmony of human appearances and the inconsistency of dark levels, the positions of eyes, noses, and mouths are situated by applying the Sobel edge administrator and locale marking in the above strategies.

Kiran *et al.* [14] proposed Second order Image Compressed and Fuzzy Reduced Grey level (SICFRG) model which reduces the dimensionality of the image and also reduces the grey level range while preserving the important feature values. The SICFRG was done in three steps. The 5×5 sub image is reduced into a 2×2 sub image with preserving the primitives, the significant attributes and any other local properties of each local sub-window. In the second step, Fuzzy rules are applied to reduce the Gray level range of compressed model of the first step. In the last step, Grey Level Co-occurrence Matrix (GLCM) is derived from second step and the GLCM features of the image are extracted. This method also classifies the facial image into 5 classes and the method is applied only on 1502 sample facial images. The average efficiency of proposed method is about 96.12%.

Murty *et al.* [24] inferred Transition based Fuzzy LBP" (TFLBP) strategy for the grouping of facial picture into five age gathering classes: youngster, youthful grown-ups, moderately aged, senior age and senior natives. The proposed TFLBP technique utilized Fuzzy surface unit on LBP idea and determined two different LBP unit values with four pixels i.e., four-joined pixels of cross inclining and four-non associated corner pixels of cross slanting of FLBP. From these particular FLBPs, the moves are checked. Based on this count, information image is classified as one of the classes specified above. The proposed method was applied on 1602 images and the efficiency got is about 96.12%.

Kumar *et al*. [16] proposed Topological Texture Features (TTF). Based on the TTF, facial image is classified into five classes: child, young adult, middle-aged, senior aged and senior citizen. The authors derived TTF's on Second order Image Compressed and Fuzzy Reduced Grey level (SICFRG) approach. The proposed approach reduced the size of the image into 1/3 rd of the original image. The proposed method is unspecified in that bone essential changes do not happen after the human is fully grown, which means that the geometric relationships of primary facial appearance do not vary. That is the reason secondary features i.e., TTF's are identified and oppressed. The proposed method was also applied on 1602 image and the average efficiency got was about 96.17%. The literature classifies the human age up to 5 categories only. No study is attempted to classify the human age into six categories. The present method has achieved this on this point. The present paper identified diamond patterns on Third Order Four pixel Pattern (TOFP). This method applies the reduction of dimensionality original image without losing the significant information of the facial image. The proposed method, which extracts the local texture features on GLCM which generates from the relative frequencies of diamond patterns, overcomes the drawbacks of original GLCM which has a size of 256×256. In this method, the size of the GLCM is only 16×16 and is more robust for age classification.

The present paper is organized as follows. The proposed methodology is described in section 2. Section 3 deals with results and discussions and comparison to other existing methods and finally in section 4, the conclusion of the present approach is discussed.

2. Methodology

2.1. Different Orders of 4-Neighborhood

One of the most important tasks in image understanding is a categorization system. The primary purpose of image understanding is to extract information from the images to allow the discrimination among different objects of interest. The classification process is usually based on grey level intensity (pixel valve), color, shape or texture. Image classification is of great interest in a variety of applications, for instance analysis of aerial satellite multi-spectral and medical images. Most of the image analysis problems are related to the properties of neighborhood pattern i.e., edge detection techniques, Texture Unit (TU), segmentation problem, dilation of image, closing operation on image, opening operation on image, LBP and etc. In a neighborhood pattern, each pixel or image values is considered as an arbitrary variable, x_r, which can undertake values x_r € {0, 1…N-1}, where N is the number of grey-level values of the image. The probability P ($x_r = x_r|$ r), where r is the neighbor set for the element x_r. The Figure 1 shows the available neighborhood orders with a central pixel. Up to now, second order neighborhood is involved in the image processing research because the center pixel is well connected with 8- neighboring pixels. The present chapter, considering the difficulties and complexities involved in the third order neighborhood, derived a new, simple and efficient model for image analysis based on transitions.

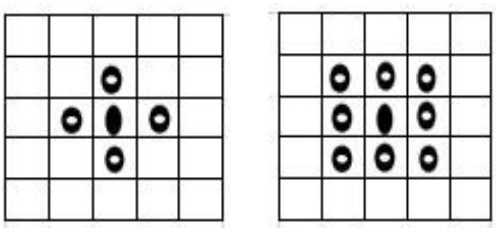

a) First Order neighbourhood pattern. b) Second order neighbourhood pattern.

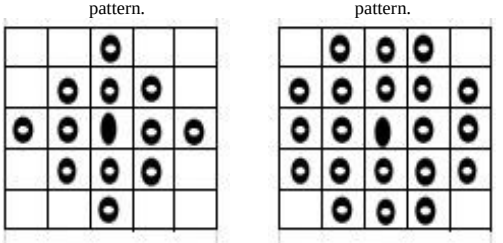

c) Third order neighbourhood pattern. d) Fourth order neighbourhood pattern.

Figure 1. Neighbourhood patterns with central pixel.

2.2. Derivation of Four Pixel Diamond Pattern Grey Level Co Occurrences Matrix (FPDP-GLCM) Of (TOFP)

FPDP-GLCMderives co-occurrences matrix based on the pixel values at Outer Diamond Corner Pixels (ODCP) of TOFP and Inner Diamond Corner Pixels (IDCP) of TOFP. The GLCM features on ODCP and IDCP of TOFP. The proposal technique consists of seven stepladders as explained below. Sometimes the human face image may be obtained in very high resolution. In such cases, the performance of the proposed method may degrade. To improve the quality or better classification results of the proposed method, wavelet concept is applied to the facial image. The image resolution is reduced when wavelets are applied so that computational cost is reduced as well. The wavelet methods [1, 13, 18, 23, 28] recommended that computational cost advantages over other methods for texture image segmentation and classification. In our proposed method, it is integrated with wavelets for classifying human age into different age groups. The block illustration of the proposal method is shown in Figure 2.

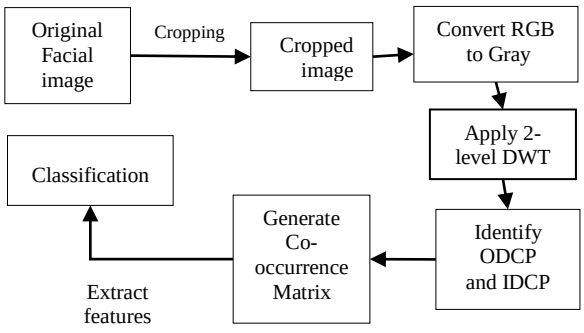

Figure 2. Block diagram of the proposal system.

The input facial image is cropped to cover the entire skin area of the face based on the location of two eyes in the first step as shown in Figure 3. The step 2 explains the conversion procedure for the RGB facial image into grey level image using HSV colour model. The Wavelet image is generated from the grey level image as explained in step 3. The pixel values are identified at the IDCP and ODCP in the fourth step. In the fifth step, Co-occurrence Matrix (CM) is formed on relative frequencies in the ODCP and IDCP patterns. In the sixth step, statistical features are extracted and evaluated on the new CM for age group classification. In the last step is derived an algorithm to categorize the facial image into one of the six categories i.e., Child: 0-9 years, Adolescents: 10-19 years, Young Adult: 20-35 years, Middle-Aged Adults: 36-45 years, Senior Adults 46- 60 years, Senior Citizen: age > 60.

a) original image. b) cropped image.

Figure 3. Image cropping.

2.3. Generation of Wavelet Image

In this proposed method, wavelet concept is applied after the conversion of RGB image into grey level image. The word wavelet is popularized by Morlet and Grossmann in the early 1980s. Today, wavelets assume a huge part in Astronomy, Acoustics, Nuclear Engineering, Sub-band Coding, Signal and Image Processing, Neurophysiology, Music, Magnetic Resonance Imaging, Speech Discrimination, Optics, Turbulence, Earthquake Prediction, Radar, Computer and Human Vision, Data Mining and Pure Mathematics Applications. They are also used for solving Partial Differential Equations.

The most generally utilized changes are the Discrete Cosine Transform (DCT), Discrete Fourier Transform (DFT), Discrete Wavelet Transform (DWT), Discrete Laguerre Transform (DLT) and the Discrete Hadamard Transform (DHT). The present strategy received DWT methods to accomplish better execution. DWT is an effective apparatus of sign and picture handling that has been effectively utilized as part of numerous experimental fields: for example, sign preparing, picture pressure, picture division, PC illustrations, and example acknowledgment. The DWT based calculations have been developed as another proficient instrument for picture handling, predominantly because of its capacity to show picture at distinctive resolutions and to accomplish higher pressure proportion. Haar wavelet is one of the most seasoned and easiest wavelets. In this way, any examination of wavelets begins with the Haar wavelet. The Haar, Daubechies, Symlets and Coiflets are minimalistic ally bolstered orthogonal wavelets.

The picture is really disintegrated i.e., separated into four sub-groups and sub-tested by applying DWT as demonstrated in Figure 4-a). These sub-groups are named LH1, HL1 and HH1. It refers to the finest scale wavelet coefficients i.e., point of interest pictures while the sub-band LL1corresponds to coarse level coefficients i.e., estimate picture. To get the following coarse level of wavelet coefficients, the sub-band LL1 alone is further deteriorated and discriminatingly inspected. The outcome of the two-level wavelet disintegration is demonstrated in Figure 4-b). Thus, to get further decay, LL2 will be utilized. This procedure proceeds until some last scale is deduced. In this paper, Haar wavelet, Daubechies wavelets, and Symlet wavelet are utilized for deterioration up to second level.

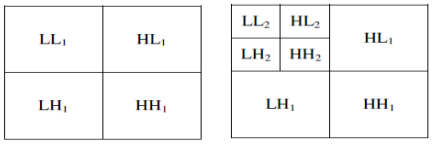

a) First level of DWT. b) Second level of DWT.

Figure 4. DWT Decomposition.

2.4. Identification of ODCP and IDCP and Generate the CM

The following procedure was adopted for identification of ODCP and IDCP and for generating the CM based on the values of IDCP and ODCP. The proposed method evaluated four pixel diamond patterns on each 5×5 facial sub image. From the Figure 1-c it is observed that the third order neighborhood includes only 13 pixels out of 25 pixels in 5×5 facial sub image. The third step contains the following sub steps.

- Each 5×5 facial sub window grey level facial image is converted into two valued (1/0) image by comparing the each pixel value of 5×5 sub window with the mean value of entire 5×5 sub window. The Equation (1) is used for converting the image into binary image.

$$P_i = \begin{Bmatrix} 0 & if & P_i < V_0 \\ 1 & if & P_i \geq V_0 \end{Bmatrix} for \quad i = 1,2,...25 \qquad (1)$$

Where V_0 the mean of the entire 5×5 sub window and Pi is the pixel value at each location of 5×5 sub window.

- The third order neighbourhood will have 2 four pixel diamond patterns. The present study named them as ODCP and IDCP. The considered patterns contain only four pixels. For visual purpose, ODCP positions are coloured by green and IDCP positions are coloured by sky blue. The resultant image is shown in the Figure 5. The Pixels P1, P5, P13 and P9 form ODCP of TOFP and the pixels P3, P6, P11 and P8 form BCP of TOFP.

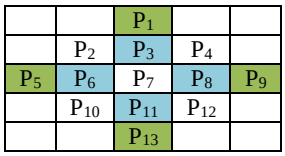

Figure 5. Considered diamond patterns.

- Considering the ODCP bit pattern, it starts from the position P1 in a clock wise direction on each 5×5 sub window. The considered bit pattern is [P1 P9 P13 P5] and calculates the corresponding decimal value. In the similar way, consider IDCP bit pattern starting from the position P3 in a clock wise direction on each 5×5 sub window. The considered bit pattern is [P3 P8 P11 P6] and calculates the corresponding decimal value. To achieve rotational invariance, both patterns in same direction are considered i.e., either clockwise or anti-clockwise direction. The resultant decimal value ranges from 0 to 15.
- The Wavelet based on Four Pixel Diamond Pattern Grey Level Co-occurrence Matrix (WFPDP-GLCM) of TOFP is generated by representing the ODCP pattern values on X-axis and IDCP pattern values on Y-axis. Generally the dimension of GLCM is about 256×256 because the distinct values in the grey level image are 256. The novelty of the present method has no standard method to use for generating concurrence matrix so that the computational cost is reduced drastically. This method has the elements of comparative frequencies in both patterns, since the decimal values of these patterns i.e., ODCP and IDCP ranges from 0 to 15. That is the reason for the WFPDP-GLCM of TOFP to have a fixed size of 16×16 because of number of distinct values in this method is 16.

2.5. Features Extraction form WFPDP-GLCM

From the generated WFPDP-GLCM the inertia, energy, homogeneity, and correlation features of TOFP have been extracted by using Equations (2, 3, 4, and 5) respectively. Based on four feature [11] values extracted from WFPDP-GLCM of facial images, an algorithm is designed to classify facial images as one of the category (Child: 0-9 years, Adolescents: 10-19 years, Young Adult: 20-35 years, Middle-Aged Adults: 36-45 years, Senior Adults 46-60 years, Senior Citizen: age > 60).

$$Inertia = \sum_{i,j=0}^{N-1} P_{i,j}(i-j)^2 \qquad (2)$$

$$Energy = \sum_{i,j=0}^{N-1} -\ln(P_{ij})^2 \qquad (3)$$

$$Local\ Homogenity = \sum_{i,j=0}^{N-1} \frac{P_{i,j}}{1+(i-j)^2} \qquad (4)$$

$$Correlation = \sum_{i,j=0}^{N-1} P_{i,j} \frac{(i-\mu)(j-\mu)}{\sigma^2} \qquad (5)$$

3. Results and Discussions

Among numerous accessible face databases around the globe [10], four of them are considered as things that incorporate huge sets of images for testing the proposed method. The MORPH Database [11] is made out of more than 17,000 pictures of about 4,000 people, between 15-68 age of males and females. The second considered database is Face and Gesture Recognition Research Network (FG-NET) ageing database. FG-NET database is made out of more than 1002 pictures of more than 80 people, from the ages of 0-69 years. And 500 pictures of 50 people from Google database. 600 pictures gathered from the scanned photos in the age range from 0 to 80. This leads to a sum of 19102 example facial pictures. In the proposed system, the test pictures are classified into six age groups of (Child: 0-9 years, Adolescents: 10-19 years, Young Adult: 20-35 years, Middle-Aged Adults: 36-45 years, Senior Adults 46-60 years, Senior Citizen: age > 60). Some of the images from different data bases are shown in Figure 6. The statistical features values of images in six age groups in different databases are listed out in Tables 1 to 6. Based on feature values in tables, an algorithm 1 is designed by the present research to classify the facial image into one of the category of Child: 0-9 years, Adolescents: 10-19 years, Young Adult: 20-35 years, Middle-Aged Adults: 36-45 years, Senior Adults 46-60 years, Senior Citizen: age> 60. After developing the algorithm to find out the efficiency of the proposed method, some facial images are considered as test images and the features on them using the proposed method is derived. Based on the proposed age classification algorithm, the age group of the test images is found. It is also checked whether they are correctly classified. Some of the test images classification results are shown in Table 7.

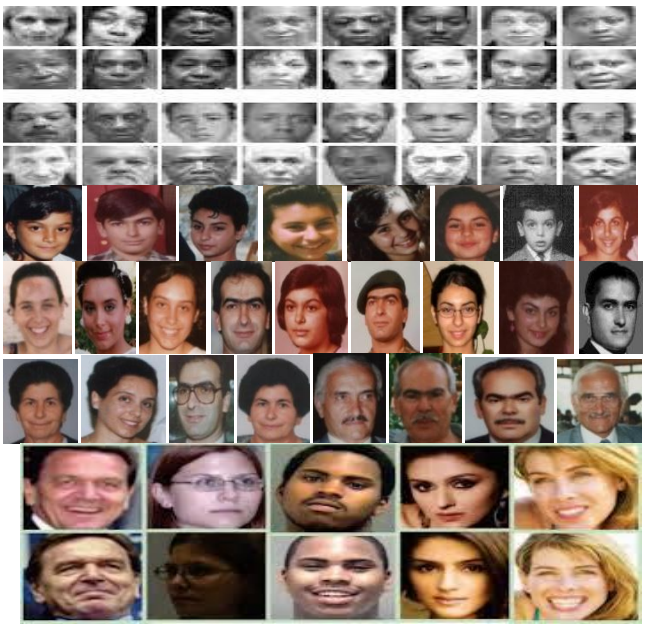

Figure 6. Sample database of facial image with different age groups.

Table 1. Statistical values of WFPDP-GLCM of TOFP for child (0-9) age images.

Sno	Image Name	Inertia	Correlation	Homogeneity	Energy
1	001A00	13.272	0.6698	0.56295	0.02523
2	010A01	47.112	0.56015	0.55107	0.02784
3	000A02	48.128	0.646	0.51516	0.01392
4	021A03	45.392	0.43605	0.43542	0.01131
5	003A04	47.176	0.5882	0.52866	0.02349
6	gi009	51.656	0.6001	0.5436	0.02697
7	gi007	55.032	0.60605	0.53631	0.0174
8	gi005	53.48	0.5576	0.50733	0.02088
9	gi004	34.808	0.56355	0.43416	0.00957
10	gi005	50.592	0.65195	0.58509	0.0348
11	si005	49.08	0.4726	0.43857	0.01044
12	si009	50.76	0.4896	0.39375	0.02001
13	si007	51.8	0.5321	0.41625	0.01566
14	si008	34.808	0.48365	0.43416	0.00957
15	si004	32.606	0.58365	0.53416	0.01275

Table 2. Statistical values of WFPDP-GLCM ofTOFP for adolescents (10-19) age images.

Sno	Image Name	Inertia	Correlation	Homogeneity	Energy
1	009A13	59.224	0.3451	0.22329	0.016095
2	001A14	103.848	0.3621	0.26982	0.021315
3	002A15	101.968	0.3094	0.21825	0.018705
4	001A16	99.232	0.33745	0.26676	0.025665
5	001A18	97.4	0.34085	0.22167	0.016965
6	011A17	101.552	0.15725	0.13914	0.010875
7	001A19	96.104	0.24905	0.17154	0.014355
8	gi016	96.848	0.1666	0.15021	0.012615
9	gi013	98.12	0.25755	0.20808	0.018705
10	gi018	96.848	0.22525	0.22419	0.024795
11	gi012	90.76	0.26945	0.2358	0.020445
12	si015	89.088	0.15725	0.14337	0.011745
13	si017	88.2768	0.21165	0.2043	0.018705
14	si019	86.952	0.18615	0.12429	0.010005
15	si015	94.048	0.2856	0.22158	0.019575

Table 3. Statistical values of WFPDP-GLCM of TOFP for young adult age images.

Sno	Image Name	Inertia	Correlation	Homogeneity	Energy
1	003A25	102.048	0.3349	0.34111	0.022185
2	012A21	102.368	0.2142	0.28639	0.016095
3	012A23	99.304	0.36635	0.35137	0.021315
4	012A24	99.88	0.34425	0.28315	0.027405
5	027A22	99.656	0.2584	0.27118	0.014355
6	011A20	96.36	0.26605	0.30943	0.018705
7	gi020	98.872	0.18445	0.30368	0.007395
8	gi020	93	0.30175	0.34507	0.023925
9	gi022	95.8	0.18615	0.33518	0.010875
10	gi025	87.12	0.3995	0.28584	0.024795
11	gi021	86.288	0.1122	0.30206	0.009135
12	si021	90.76	0.17595	0.27395	0.011745
13	si025	88.36	0.2261	0.31209	0.013485
14	si024	90.792	0.2431	0.29638	0.016965
15	001A33	104.824	0.26945	0.46998	0.01392

Table 4. Statistical values of WFPDP-GLCM of TOFP for middle-aged adults images.

Sno	Image Name	Inertia	Correlation	Homogeneity	Energy
1	001A40	92.064	0.35615	0.51489	0.01392
2	003A38	95.128	0.42245	0.55944	0.00957
3	019A37	92.528	0.3757	0.52515	0.01566
4	020A36	93.04	0.29155	0.48537	0.01044
5	021A39	96.456	0.3672	0.50742	0.00957
6	001A43	94.104	0.19295	0.49438	0.00696
7	gi040	100.2	0.36975	0.53262	0.01392
8	gi042	98.016	0.37825	0.52308	0.01305
9	gi045	84.6	0.34765	0.51138	0.01305
10	gi042	86.8	0.2975	0.48537	0.01305
11	si039	98.832	0.2737	0.56314	0.01392
12	si045	95.648	0.2516	0.54757	0.01392
13	si038	95.008	0.2261	0.4988	0.01479
14	si041	91.592	0.3332	0.50319	0.01305
15	si044	97.384	0.16745	0.5762	0.00696

Table 5. Statistical values of WFPDP-GLCM of TOFP for senior adults age images.

Sno	Image Name	Inertia	Correlation	Homogeneity	Energy
1	003A51	130.736	0.35820275	0.49878	0.017139
2	003A57	128.912	0.39279605	0.56358	0.030363
3	003A58	131.592	0.35846285	0.55773	0.033321
4	003A59	131.968	0.4159662	0.51128	0.03132
5	003A60	132.736	0.3165893	0.46836	0.015312
6	gi052	128.688	0.3070846	0.46854	0.01479
7	gi055	125.248	0.3558032	0.50229	0.022272
8	gi052	133.224	0.3673224	0.53973	0.029145
9	gi055	134.936	0.2738547	0.4491	0.014094
10	gi060	126.048	0.32121245	0.46323	0.02175
11	si049	134.072	0.3143742	0.52929	0.0261
12	si051	134.789	0.28533395	0.54189	0.02262
13	si058	130.288	0.2945131	0.5319	0.0261
14	si059	132.2	0.2673811	0.51732	0.02436
15	si055	133.888	0.3515515	0.42966	0.03306

Table 6. Feature set values of WFPDP-GLCM of TOFP for senior citizens age images.

Sno	Image Name	Inertia	Correlation	Homogeneity	Energy
1	006A69	61.928	0.104975	0.39835	0.03567
2	003A61	50.144	0.201025	0.39304	0.04089
3	004A53	60.144	0.14926	0.31204	0.03567
4	004A62	60.856	0.38777	0.32212	0.037932
5	004A63	52.384	0.385135	0.41058	0.04176
6	gi066	51.48	0.38828	0.33112	0.039672
7	gi068	60.048	0.39933	0.41276	0.036975
8	gi065	55.008	0.3711015	0.32076	0.03741
9	gi062	61.512	0.29971	0.48932	0.040281
10	gi062	58.624	0.390116	0.46107	0.039324
11	si069	59.648	0.39797	0.31204	0.0366531
12	si061	55.632	0.3943065	0.29304	0.040716
13	si068	54.024	0.21131	0.38079	0.0392544
14	si069	56.448	0.36006	0.29331	0.038454
15	si070	54.872	0.3673275	0.32931	0.037584

Table 7. Some of the test set results of the WFPDP-GLCM-TOFP method.

Sno	Image	Energy	Correlation	Inertia	Homogeneity	Group	Result
1	gog_i_01	0.42333	0.4592	51.464	0.0087	Child	Correct
2	goge_i_02	0.4491	0.2738547	130.424	0.014964	Senior Adult	Correct
3	gog_i_03	0.32931	0.3673275	54.872	0.037584	Senior Citizen	Correct
4	gog_i_04	0.2358	0.26945	90.76	0.020445	Adolescents	Correct
5	gogi_05	0.57457	0.2516	105.648	0.01392	Middle Aged Adult	Correct
6	gog_i_06	0.47124	0.30532	61.232	0.043761	Senior Citizen	Correct
7	gog_i_07	0.47718	0.3317134	133.792	0.016008	Senior Adult	Correct
8	gog_i_08	0.4988	0.2161	102.008	0.01479	Middle Aged Adult	Correct
9	gog_i_09	0.46998	0.22945	94.824	0.01392	Young Adult	Correct
10	gog_im10	0.28396	0.49815	83.872	0.00261	Adolescents	Correct
11	066A54	0.46323	0.3212125	126.048	0.02175	Senior Adult	Correct
12	067A00	0.51509	0.67195	52.592	0.0348	Child	Correct
13	082A20	0.42597	0.2562	96.664	0.01305	Young Adult	Correct
14	072A25	0.35629	0.27407	109.272	0.01479	Young Adult	Correct
15	077A53	0.47718	0.3317134	131.04	0.016008	Senior Adult	Correct
16	077A29	0.29638	0.2331	96.792	0.016965	Young Adult	Correct
17	058A45	0.53614	0.2737	108.832	0.01392	Middle Aged Adult	Correct
18	058A14	0.27488	0.38615	77.648	0.023925	Adolescents	Correct
19	077A48	0.46323	0.3212125	126.048	0.02175	Senior Adult	Correct
20	058A65	0.32212	0.38777	60.856	0.037932	Senior Citizen	Correct
21	sca.im-001	0.50045	0.60815	54.872	0.02349	Child	Correct
22	sca.im-002	0.45837	0.2975	96.8	0.01705	Middle Aged Adult	Correct
23	sca.im-003	0.43151	0.4041	50.728	0.01653	Child	Correct
24	sca.im-004	0.567	0.04531	110.328	0.03229	Senior Adult	Wrong
25	sca.im-005	0.41112	0.225165	59.16	0.040716	Senior Citizen	Correct
26	sca.im-006	0.32109	0.2161	98.36	0.013485	Young Adult	Correct
27	sca.im-007	0.21545	0.50015	84.464	0.01566	Adolescents	Correct
28	sca.im-008	0.21158	0.3156	84.048	0.019575	Adolescents	Correct
29	sca.im-009	0.46836	0.3165893	131.736	0.015312	Senior Adult	Correct
30	sca.im-010	0.51138	0.34765	94.6	0.01605	Middle Aged Adult	Correct

Algorithm 1:Facial Image age-group classification based on values derived from WFPDP-GLCM of TOFP

BEGIN
if Inertia > 125 then
Facial image is treated as "Senior Adult (46-60) group"
Otherwise if Inertia < 125 and Homogeneity <= 0.2698 then
Facial image is treated as "Adolescents (10-19) group"
Otherwise if Inertia<125 and Energy > 0.03567 then
Facial image is treated as "Senior Citizen Age (>60) group"
Otherwise if Inertia < 55.032 and Correlation > 0.436 then
Facial image is treated as "child Age (0-9) group"
Otherwise if Inertia > 75.6 and Correlation <= 0.47808 then
Facial image is treated as "Young Adult (20+35) group"
Otherwise if Inertia > 75.6 and Correlation > 0.48 then
Facial image is treated as "Middle age (36+45) group"
Otherwise
Facial image is treated as Unknown Class

3.1. Analysis of the Proposed Method

To analyze the proficiency of the proposed system, the outcomes of the proposed method are analyzed in two ways. The first way is called Response Result Analysis (RRA) approach and another way is gotten Ten Cycle Cross Validation (TCCV) approach.

- *Response Result Analysis (RRA) approach*: In RRA, Entire dataset of some of the images is treated as a test set i.e., 600 images from FG-NET data base, 1500 images from Morph data base, 400 images from Google and 300 images from scanned images. It leads to a total of 2800 images. Calculating the feature values by the proposed method and grouping the images based on the proposed derived algorithm1. The % of grouping and grouping results of the images in the test database are listed out in the Tables 8, 9, 10, and 11 respectively. The mean percentage grouping of the Response Result Analysis approach for the test database is listed out in Table 12. The classification graph of the test database in RRA is shown in Figure 7.

Table 8. % of group results of the fg-net database.

Class	FG-Net Database			
	Total	**Properly classified**	**not correctly classified**	**% of Classification**
Child	85	84	1	98.82
Adolescents	92	90	2	97.83
Young Adult	96	94	2	97.92
Middle Aged Adult	123	120	3	97.56
Senior Adult	100	98	2	98.00
Senior Citizen	104	101	3	97.12

Table 9. % of group results of the morph database.

Class	Morph database			
	Total	**Properly classified**	**not correctly classified**	**% of Classification**
Child	235	232	3	98.72
Adolescents	237	233	4	98.31
Young Adult	272	269	3	98.90
Middle Aged Adult	265	262	3	98.87
Senior Adult	243	240	3	98.77
Senior Citizen	248	244	4	98.39

Table 10. % of group results of the google database.

Class	Google Images			
	Total	Properly classified	notcorrectl yclassified	% of Classification
Child	73	71	2	97.26
Adolescents	78	75	3	96.15
Young Adult	68	65	3	95.59
Middle Aged Adult	63	61	2	96.83
Senior Adult	57	55	2	96.49
Senior Citizen	61	58	3	95.08

Table 11. % of group results of the scanneddatabase.

Class	Scanned Images			
	Total	Properly classified	not correctly classified	% of Classification
Child	43	41	2	95.35
Adolescents	47	43	4	91.49
Young Adult	55	51	4	92.73
Middle Aged Adult	48	44	4	91.67
Senior Adult	58	53	5	91.38
Senior Citizen	49	45	4	91.84

Table 12. Overall % of group results of the RRA approach.

Class	% of Classification in RRA Approach			
	Fg-Net	Morph	Google	Scanned
Child	98.82	98.72	97.26	95.35
Adolescents	97.83	98.31	96.15	91.49
Young Adult	97.92	98.90	95.59	92.73
Middle Aged Adult	97.56	98.87	96.83	91.67
Senior Adult	98.00	98.77	96.49	91.38
Senior Citizen	97.12	98.39	95.08	91.84

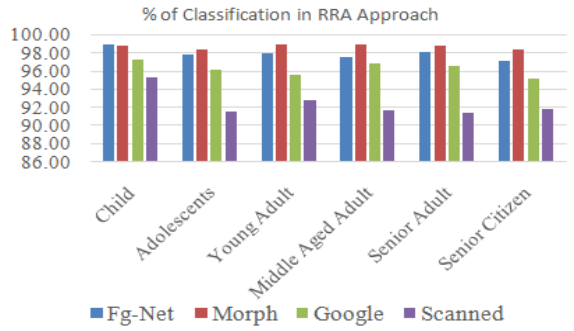

Figure 7. Classification graph of the RRA Approach.

From the RRA approach we observe that the scanned images have got less percentage of classification compared to all other databases. The scanned image quality depends on the scanner and also on the hard copy of the image. The images are scanned by scanner in 300 dpi. If quality increases, percentage of classification may be increased.

- *Ten Cycle Cross Validation (TCCV) approach*: In TCCV approach results analysis strategy, the data base is divided into 10 sets i.e., each set consists of 280 images. Each set is a mix up with the images of Fg-Net data base, Morph data base, Google images, and Scanned images. Every set must contain six classes of age groups i.e., child, adolescents, young adults, middle aged adults, senior adults, Senior citizens. In TCCV approach, results are analyzed in 10 Cycles. In cycle 1, first set is treated as a test set and remaining nine sets are taken as a sample dataset. Compute the % of image grouping for test set. In cycle 2, second set is dealt with as a test set and staying nine sets are taken as sample information. Computing the % of grouping for test set, same methodology is applied for remaining cycles also. This approach strengthened the proposed method. The % of image grouping of the proposed strategy in ten cycles is listed in Tables 13 to 22 individually. The overall % of image grouping of the TCCV strategy is shown in Table 23 and 24 and relating grouping chart in indicated in Figure 8.

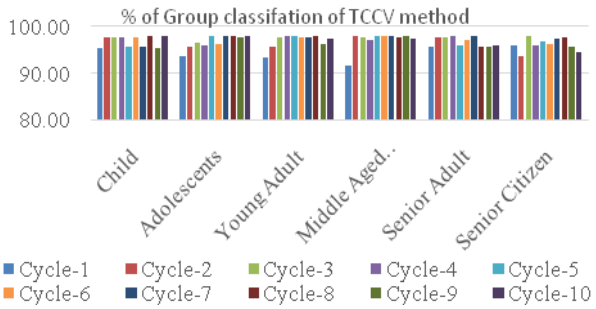

Figure 8. Cycle wise classification graph of TCCV method.

Table 13. % of image grouping of the proposed method in cycle-1 of TCCV approach.

Class	Cycle 1			
	Total	Properly classified	not correctly classified	% of Classification
Child	43	41	2	95.35
Adolescents	47	44	3	93.62
Young Adult	45	42	3	93.33
Middle Aged Adult	48	44	4	91.67
Senior Adult	48	46	2	95.83
Senior Citizen	49	47	2	95.92

Table 14. % of image grouping of the proposed method in cycle-2 of TCCV approach.

Class	Cycle 2			
	Total	Properly classified	not correctly classified	% of Classification
Child	45	44	1	97.78
Adolescents	46	44	2	95.65
Young Adult	47	45	2	95.74
Middle Aged Adult	49	48	1	97.96
Senior Adult	45	44	1	97.78
Senior Citizen	48	45	3	93.75

Table 15. % of image grouping of the proposed method in cycle-3 of TCCV approach.

Class	Cycle 3			
	Total	Properly classified	not correctly classified	% of Classification
Child	44	43	1	97.73
Adolescents	57	55	2	96.49
Young Adult	44	43	1	97.73
Middle Aged Adult	43	42	1	97.67
Senior Adult	45	44	1	97.78
Senior Citizen	47	46	1	97.87

Table 16. % of image grouping of the proposed method in cycle-4 of TCCV approach.

Class	Cycle 4			
	Total	Properly classified	not correctly classified	% of Classification
Child	46	45	1	97.83
Adolescents	51	49	2	96.08
Young Adult	49	48	1	97.96
Middle Aged Adult	36	35	1	97.22
Senior Adult	48	47	1	97.92
Senior Citizen	50	48	2	96.00

Table 17. % of image grouping of the proposed method in cycle-5 of TCCV approach.

Class	Cycle 5			
	Total	Properly classified	not correctly classified	% of Classification
Child	47	45	2	95.74
Adolescents	52	51	1	98.08
Young Adult	48	47	1	97.92
Middle Aged Adult	51	50	1	98.04
Senior Adult	50	48	2	96.00
Senior Citizen	32	31	1	96.88

Table 18. % of image grouping of the proposed method in cycle-6 of TCCV approach.

Class	Cycle 6			
	Total	Properly classified	not correctly classified	% of Classification
Child	44	43	2	97.73
Adolescents	54	52	2	96.30
Young Adult	46	45	4	97.83
Middle Aged Adult	48	47	1	97.92
Senior Adult	35	34	1	97.14
Senior Citizen	53	51	2	96.23

Table 19. % of image grouping of the proposed method in cycle-7 of TCCV approach.

Class	Cycle 7			
	Total	Properly classified	not correctly classified	% of Classification
Child	48	46	1	95.83
Adolescents	51	50	1	98.04
Young Adult	46	45	1	97.83
Middle Aged Adult	47	46	1	97.87
Senior Adult	51	50	1	98.04
Senior Citizen	37	36	1	97.30

Table 20. % of image grouping of the proposed method in cycle-8 of TCCV approach.

Class	Cycle 8			
	Total	Properly classified	not correctly classified	% of Classification
Child	49	48	1	97.96
Adolescents	47	46	1	97.87
Young Adult	53	52	1	98.11
Middle Aged Adult	42	41	1	97.62
Senior Adult	46	44	2	95.65
Senior Citizen	43	42	1	97.67

Table 21. % of image grouping of the proposed method in cycle-9 of TCCV approach.

Class	Cycle 9			
	Total	Properly classified	not correctly classified	% of Classification
Child	43	41	2	95.35
Adolescents	42	41	1	97.62
Young Adult	52	50	2	96.15
Middle Aged Adult	49	48	1	97.96
Senior Adult	46	44	2	95.65
Senior Citizen	48	46	2	95.83

Table 22. % of image grouping of the proposed method in cycle-10 of TCCV approach.

Class	Cycle 10			
	Total	Properly classified	not correctly classified	% of Classification
Child	51	50	1	98.04
Adolescents	49	48	1	97.96
Young Adult	37	36	1	97.30
Middle Aged Adult	39	38	1	97.44
Senior Adult	49	47	2	95.92
Senior Citizen	55	52	3	94.55

Table 23. Cycle wise % of image grouping in TCCV approach.

Class	Cycle-1	Cycle-2	Cycle-3	Cycle-4	Cycle-5
Child	95.35	97.78	97.73	97.83	95.74
Adolescents	93.62	95.65	96.49	96.08	98.08
Young Adult	93.33	95.74	97.73	97.96	97.92
Middle Aged Adult	91.67	97.96	97.67	97.22	98.04
Senior Adult	95.83	97.78	97.78	97.92	96
Senior citizen	95.92	93.75	97.87	96	96.88
Class	Cycle-6	Cycle-7	Cycle-8	Cycle-9	cycle-10
Child	97.73	95.83	97.96	95.35	98.04
Adolescents	96.3	98.04	97.87	97.62	97.96
Young Adult	97.83	97.83	98.11	96.15	97.3
Middle Aged Adult	97.92	97.87	97.62	97.96	97.44
Senior Adult	97.14	98.04	95.65	95.65	95.92
Senior citizen	96.23	97.3	97.67	95.83	94.55

From the above ten cycles cross validation approach, the mess matrix is made which represents the overall accuracy of the proposed approach described effectively and clearly. The mess matrix represents the classification relationship between the facial image groups. That means it shows how many facial images are classified correctly into a particular age group. This mess matrix also displays how many facial images are not correctly classified and in which category they are classified. The resultant mess matrix is listed in Table 24.

Table 24. Mess matrix of the proposed method.

		Classified Group					
	Class	Child	Adolescents	Young Adult	Middle Aged Adult	Senior Adult	Senior Citizen
ORIGINAL	Child	446	3	2	2	3	4
	Adolescents	3	480	3	4	1	5
	Young Adult	4	5	450	3	2	3
	Middle Aged Adult	1	3	4	439	2	3
	Senior Adult	3	2	3	4	448	3
	Senior Citizen	2	5	3	4	4	444

4. Comparisons Of The Proposed Method With Other Existing

From Table 7, it is observed that the efficiency of the proposed technique is praiseworthy. To assess the effectiveness of the proposed technique, it is compared to other age estimation methods [15, 27]. The strategy proposed by Kumar *et al*. [15] the facial image is classified into four age groups in view of incorporating the highlights got from Gray Level Co-occurrence Matrix (GLCM) and four distinctive LBP's (4-DLBP) on a 3×3 sub window got from another basic methodology. The age group classification strategy proposed by Thakur and Verma [27] facial images are categorized into four age groups using Neural Network with back propagation. The classification rate of proposal system and other existing techniques are listed in Table 25. The graphical representation of the rate mean grouping rate for the proposed system and other existing method are demonstrated in Figure 9.

Table 25. % rate of success of the proposed FPDP-GLCM-TOFP method and other active methods.

sno	Data Base	Integrated Approach	NN with back propagation algorithm.	Proposed WFPDP -GLCM Method
1	FG-Net	93.23	89.25	96.5
2	Scanned Images	92.5	88.65	97.76
3	Google	91.5	90.15	96.98
4	MORPH Database	91.75	90.64	97.57

The Table 25 clearly indicates that the proposed WFPDP-GLCM Method outperforms the other existing methods. Figure 9 shows the comparison chart of the proposed Wavelet based on Four Pixel Diamond Pattern Grey Level Co-occurrence Matrix (WFPDP-GLCM) method with the other existing methods of Table 25.

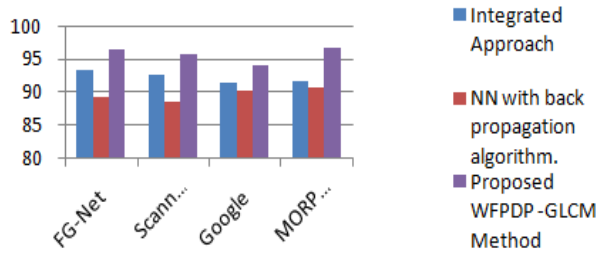

Figure 9. % of rate of success chart proposed WFPDP-GLCM method and other existing methods.

5. Conclusions

The proposed method assessed the relationship between the outer diamond and Inner diamond corner pixels of TOFP. The proposed method utilizes the advantages of the wavelet concept to reduce the dimensionality of the image and also that causes reducing the computational cost. This is the first approach to classify the human age into six categories. The inner diamond corner pixels are connected component whereas the outer diamond corner pixels of TOFP are not connected component. In the proposed method successively presented and utilized the TOFP by reducing the complexity in establishing the Binary code value for 13 pixels i.e., ranges from 0 to 2^{13}-1. The novelty of the proposed method is that, the standard method is not used for generating the concurrence matrix. The novelty of the proposed method is that no standard classification algorithm is used to classify the facial image into one six categories. The efficiency of the proposed approach is high. When compared with other existing methods, the proposed method exhibits high classification rate and no method has correctly classified the human age into six categories.

References

[1] Antonini M., Barlaud M., Mathieu P., and Daubechies I., "Image Coding Using Wavelet Transform," *IEEE Transactions Image Processing*, vol. 1, no. 2, pp. 205-220, 1992.

[2] Burt D. and Perrett D., "Perception of Age in Adult Caucasian Male Faces: Computer Graphic Manipulation of Shape and Colour Information," *in Proceedings of the Royal Society of London B, B-259*, vol. 259, no. 1355, pp. 137-143, 1995.

[3] Dehon H. and Bredart S., "An other-Race Effect in Age Estimation from Faces," *Perception*, vol. 30, no. 9, pp. 1107-1113, 2001.

[4] Edwards G., Lanitis A., Taylor C., and Cootes T., "Statistical Face Models: Improving Specific City," *Image and Vision Computing*, vol. 16, no. 3, pp. 203-211, 1998.

[5] Fu Y., Guo G., and Huang T., "Age Synthesis and Estimation via Faces: A Survey," *IEEE Transactions on Pattern Analysis and Machine Intelligence*, vol. 32, no. 11, pp. 1955-1976, 2010.

[6] Gao F. and Ai H., "Face Age Classification on Consumer Images With Gabor Feature and Fuzzy LDA Method," *in Proceedings of the 3rd International Conference on Advances in Biometrics*, Alghero, pp. 132-141, 2009.

[7] Geng X., Zhou Z., Zhang Y., Li G. and Dai H., "Learning from Facial Aging Patterns for Automatic Age Estimation," *in Proceedings of 14th ACM International Conference on Multimedia*, Santa Barbara, pp. 307-316, 2006.

[8] Guo G., Fu Y., Dyer C., and Huang T., "Image-Based Human Age Estimation by Manifold Learning and Locally Adjusted Robust Regression," *IEEE Transactions on Image Processing*, vol. 17, no. 7, pp. 1178-1188, 2008.

[9] Guo G., Mu G., Fu Y., Dyer C., and Huang T., "A Study on Automatic Age Estimation Using A Large Database," *in Proceedings IEEE 12th International Conference on Computer Vision*, Kyoto, pp. 1986-1991, 2009.

[10] Haralick R., Shanmugan K., and Dinstein I., "Textural Features for Image Classification," *IEEE Transactions on Systems, Man, and Cybernetics*, vol. SMC-3, no. 6, pp. 610-621, 1973.

[11] HomePage Face Recognition, Available at: http://www.face-rec.org/databases/, Last Visited, 2014.

[12] Horng W., Lee C., and Chen C., "Classification of Age Groups Based on Facial Features," *Tamkang Journal of Science and Engineering*, vol. 4, no. 3, pp. 183-192, 2001.

[13] Khalifa O., "Wavelet Coding Designfor Image Data Compression," *The International Arab Journal of Information Technology*, vol. 2, no. 2, pp. 118-128, 2005.

[14] Kiran J., Kumar V., and Reddy B., "Age Classifications Based on Second Order Image Compressed and Fuzzy Reduced Grey Level (SICFRG) Model," *International Journal on*

Computer Science and Engineering, vol. 5, no. 06, pp. 481-492, 2013.

[15] Kumar P., Kumar V., and Venkatarao R., "Age Classification Based On Integrated Approach," *International Journal of Image, Graphics and Signal Processing*, vol. 7, pp. 50-57, 2014.

[16] Kumar V., Kiran J., and Chandana V., "An Effective Age Classification Using Topological Features Based on Compressed and Reduced Grey Level Model of the Facial Skin," *International Journal of Image, Graphics and Signal Processing*, vol. 6, no. 1, pp. 9-17, 2014.

[17] Kwon Y. and Lobo N., "Age Classification from Facial Images," *in Proceedings of IEEE Conference on Computer Vision and Pattern Recognition*, Seattle, pp. 762-767, 1994.

[18] Laine A. and Fan J., "Texture Classification by Wavelet Packet Signatures," *IEEE Transactions on Pattern Analysis and Machine Intelligence*, vol. 15, no. 11, pp. 1186-1190, 1993.

[19] Lanitis A., Draganova C., and Christodoulou C., "Comparing Different Classifiers for Automatic Age Estimation," *IEEE Transactions on Systems, Man, and Cybernetics, Part B: Cybernetics*, vol. 34, no. 1, pp. 621-628, 2004.

[20] Lanitis A., Taylor C., and Cootes T., "Toward Automatic Simulation of Aging Effects on Face Images," *IEEE Transactions on Pattern Analysis and Machine Intelligence*, vol. 24, no. 4, pp. 442-455, 2002.

[21] Lian H. and Lu B., "Age Estimation Using A Min-Max Modular Support Vector Machine," *in Proceedings of 12th International Conference on Neural Information Processing*, Taipei, pp. 83-88, 2005.

[22] Luu K., Ricanek K., Bui T., and Suen C., "Age Estimation Using Active Appearance Models and Support Vector Machine Regression," *in Proceedings of the IEEE 3rd International Conference on Biometrics: Theory, Applications, and Systems*, Washington, pp. 1-5, 2009.

[23] Montiel E., Aguado A., and Nixon M., "Texture Classification via Conditional Histograms," *Pattern Recognition Letters*, vol. 26, no. 11, pp. 1740-1751, 2005.

[24] Murty G., Kumar V., and Obulesu A., "Age Classification Based on Simple LBP Transitions," *International Journal on Computer Science and Engineering*, vol. 5, no. 10, pp. 885-893, 2013.

[25] Shan C., "Learning Local Features for Age Estimation on Real-Life Faces," *in Proceedings of ACM International Workshop on Multimodal Pervasive Video Analysis*, Firenze, pp. 23-28, 2010.

[26] Suo J., Wu T., Zhu S., Shan S., Chen X., and Gao W., "Design Sparse Features for Age Estimation Using Hierarchical Face Model," *in Proceedings of The 8th IEEE International Conference on Automatic Face and Gesture Recognition*, Amsterdam, pp. 17-19, 2008.

[27] Thakur S. and Verma L., "Age Identification of Facial Images using Neural Network," *Journal of Computer Science and Information Technologies*, vol. 3, no. 3, pp. 4244-4247, 2012.

[28] Wouwer G., Scheunders P., Livens S., and Dyck D., "Wavelet Correlation Signatures for Color Texture Characterization," *Pattern Recognition*, vol. 32, no. 3, pp. 443-451, 1999.

[29] Yan S., Wang H., Tang X., and Huang T., "Learning Auto-Structured Regressor from Uncertain Nonnegative Labels," *in Proceedings of IEEE 11th International Conference on Computer Vision*, Rio de Janeiro, pp. 1-8, 2007.

Rajendra Chikkala received the B.Tech degree in Computer Science & Engineering from Jawaharlal Nehru Technological University, Hyderabad, India in 2005, M.Tech. degree in Computer Science and Engineering from Acharya Nagarjuna University, India in 2008, and registered for Ph.D. in Computer Science and Engineering at Jawaharlal Nehru Technological University under the guidance of Prof. E. Srinivasa Reddy and Prof. B.Prabhakara Rao. His research interests include Image Processing.

Sreenivasa Edara received the B.Tech degree in Electronics and Communication Engineering from Nagarjuna University, India in 1988, M.S. degree from Birla Institute of Technology and Science, India in 1997, M.Tech degree in Computer Science from Visveswaraiah Technological University, India in 2000 and Ph.D in computer science from Acharya Nagarjuna University, India in 2008. He is the senior member of IEEE and presented 11 papers in international conferences and 6 journal papers. Presently working as principal in ANU college of Engineering. His research interest includes image processing, biometrics and pattern recognition.

Prabhakara Bhima has more than 28 years of experience in teaching and 20 years of R & D. He is an expert in Signal Processing & Communications. He produced 6 PhD's and guiding 25 PhD scholars. He held Head of the Department, in JNTU College of Engineering. Presently working as Rector in JNTU Kakinada. He published more than 85 technical papers in national and International journals and conferences.